To cite this article: CHEN H H, ZHAO H, WANG N, et al. Accurate track control of unmanned underwater vehicle under complex disturbances [J/OL]. Chinese Journal of Ship Research, 2022, 17(2). http://www.ship-research.com/en/article/doi/10.19693/j.issn.1673-3185.02236.

DOI: 10.19693/j.issn.1673-3185. 02236

Accurate tracking control of unmanned underwater vehicles under complex disturbances

CHEN Haohua[1], *ZHAO Hong*[1], *WANG Ning*[*1, 2], *GUO Chen*[1], *LU Ting*[1], *WANG Ning*[1]

1 College of Marine Electrical Engineering, Dalian Maritime University , Dalian 116026, China

2 College of Shipbuilding Engineering, Harbin Engineering University, Harbin 150001, China

Abstract: [**Objectives**] This paper presents a non-singular terminal sliding mode track control method based on a finite-time disturbance observer to solve the problem of accurately tracking and controlling the 3D trajectory of an unmanned underwater vehicle under complex external disturbances. [**Methods**] A nonsingular terminal sliding mode track controller is designed to ensure that the tracking error converges to zero accurately within a limited time. A finite-time disturbance observer is designed to improve the anti-jamming ability of the system under external multidimensional time-varying disturbances. [**Results**] The Lyapunov function is used to prove that the designed control strategy can remain stable for a limited time. MATLAB is used for the simulation experiment, and a comparison with the backstepping sliding mode control method under step disturbance shows that the method presented in this paper achieves accurate trajectory tracking. [**Conclusions**] The results of this paper can provide a solution for accurately tracking the 3D trajectories of unmanned underwater vehicles.

Key words: unmanned underwater vehicle; 3D trajectory tracking; finite-time disturbance observer; step disturbance; nonsingular terminal sliding mode; backstepping sliding mode

CLC number: U674.941

0 Introduction

Unmanned underwater vehicles (UUVs) are intelligent underwater vehicles that can fulfill a task according to the preset instructions or the wishes of operators. They are widely used in civil and military fields, such as offshore oil and gas exploration and development, marine environmental observation, and torpedo investigation [1-3]. High-precision trajectory tracking control is the prerequisite for UUVs to fulfill these tasks and thus has attracted wide attention from scholars [4]. However, a UUV is a multi-degree-of-freedom coupled and multivariable nonlinear system. Due to the interference from the complex underwater environment such as waves, ocean currents, and collisions of marine organisms, the design of the trajectory tracking controller of UUVs faces difficulties. The controller should have the ability of nonlinearity processing and anti-jamming [5].

Sliding mode control (SMC) is not sensitive to the unmodeled part of the system and has the anti-jamming ability to some extent, so it is widely used in the field of trajectory tracking control of UUVs [6].

Received: 2020 − 12 − 23 **Accepted**: 2022 − 04 − 06

Supported by: National Natural Science Foundation of China (51579024); Foundation for Equipment Pre-research Key Laboratory (6142215200106); Foundation for "Xingliao Talent Plan" of Liaoning Province (XLYC1807013); Fundamental Research Funds for the Central Universities of China (3132019318, 3132019344)

Authors: CHEN Haohua, male, born in 1995, master degree . Research interest: trajectory tracking control of unmanned underwater vehicles. E-mail: chenhaohua0617@163.com

ZHAO Hong, born in 1967, Ph.D., professor. Research interest: electrical drive and control, marine electric propulsion, and application of intelligent control in electrical engineering. E-mail: zhaohong@dlmu.edu.cn

WANG Ning, born in 1983, Ph.D., professor. Research interest: intelligent control of marine robots, unmanned ships, and autonomous systems. E-mail: n.wang@ieee.org

***Corresponding author**: WANG Ning

Aiming at the problem of 3D trajectory tracking control of UUVs, Qiao et al. [7] proposed a double closed-loop buffeting-free adaptive SMC method to solve the problem of 3D trajectory tracking control of UUV. The outer-loop position controller and inner-loop speed controller were designed, and the saturation function was used to replace the sign function to overcome the outer-loop buffeting. In addition, a continuous adaptive term was designed to replace the discontinuous switching function of traditional sliding modes, and the global asymptotic stability of the double-loop control system was proved by the Lyapunov stability theory. Rezazadegan et al. [8] proposed an adaptive backstepping controller based on the Lyapunov direct method for the 3D trajectory tracking control of UUVs. The results showed that the actual trajectory can asymptotically converge to the desired trajectory but could not achieve finite-time stability. Guerrero et al. [9] proposed an adaptive high-order SMC method, which ignored the influence of the upper bound of the disturbance on the system while preserving the advantages of robust control. They applied this algorithm to the Leonard ROV depth trajectory tracking control and yaw control. The experimental results showed that the control strategy could effectively suppress the uncertainty of external disturbances and hydrodynamic parameters. Qiao et al. [10] proposed an adaptive nonsingular integral terminal SMC strategy for the 3D trajectory tracking control of UUVs under time-varying external disturbances. The singular problem in traditional SMC was eliminated, which ensured that the velocity tracking error locally converged to zero within a finite time, and the position tracking error locally and exponentially converged to zero. Sun et al. [11] adopted the backstepping sliding mode control (BSMC) strategy. The control strategy obtained continuous and smooth control input and effectively suppressed external disturbances. Based on the BSMC, Wei et al.[12] introduced a bio-inspired neural dynamic model to solve the problem of velocity jump in smooth output. The simulation results showed that remotely operated underwater vehicles can effectively solve the velocity jump caused by the backstepping sliding mode. Zhang et al. [13] introduced the radial basis function neural network and backstepping method to solve the tracking impact problem caused by the jump of controller motion parameters at the inflection point. Meanwhile, the singular value problem in single backstepping control was avoided. Lyapunov stability theory was used to analyze the stability of the entire closed-loop control system, but it could not achieve accurate tracking of the desired trajectory. Yan et al. [14] proposed a double closed-loop terminal SMC strategy. The negative feedback of position and attitude was taken as the outer-loop control, and the virtual speed was introduced as the desired target of the inner-loop controller. The terminal SMC method was used to reduce the buffeting and make the tracking error converge within a finite time. The simulation results showed that the control strategy could accurately track the spatial trajectory. However, its design process was complex, and the calculation burden was heavy, which could not be widely used in trajectory tracking control of UUVs. Aiming at complex external disturbances, Wang et al. [15-16] attempted to use observer technology to improve the tracking accuracy of unmanned ships and compensate for complex unknown disturbances in time to achieve accurate attitude adjustment and improve the tracking accuracy.

In terms of accurately tracking and controlling the 3D trajectory of a UUV, this paper uses a finite-time disturbance observer (FDO) to observe complex external disturbances and designs a nonsingular terminal sliding mode controller based on the finite-time disturbance observer (FDO-NTSMC) by combing the nonsingular terminal sliding mode control (NTSMC). The designed FDO can accurately observe external time-varying disturbances and lower the influence of disturbances on the system to improve the anti-jamming ability of the system, and it can reduce the buffeting generated by NTSMC based on the power reaching law. In addition, the Lyapunov function and related lemmas are used to prove that the trajectory tracking system of the UUV based on the proposed strategy can converge within a finite time. Finally, the simulation results show that the FDO-NTSMC strategy can not only achieve accurate tracking of the desired trajectory of the UUV but also has a better control performance than the BSMC strategy under complex underwater environmental disturbances such as time-varying disturbances and step superposition disturbances.

1 Preparatory knowledge and mathematical model

1.1 Preparatory knowledge

Theorem 1 [17]: in terms of the nonlinear system,

$$\dot{\boldsymbol{x}}(t) = f(x(t)) \tag{1}$$

where $\boldsymbol{x} = [x_1, \ldots, x_n]^{\mathrm{T}}$ is the n-dimensional state vector of the system; $f(\cdot)$ is a nonlinear system in the neighborhood of the origin, and $f(0)$ equals 0. If a function $\boldsymbol{V}(x, t)$ satisfies

1) $\boldsymbol{V}(x, t)$ is positive definite, and $\dot{\boldsymbol{V}}(x,t)$ is negative definite, then the system is asymptotically stable at the origin.

2) $\boldsymbol{V}(x, t)$ is positive definite, and $\dot{\boldsymbol{V}}(x,t)$ is negative semidefinite, with $\dot{\boldsymbol{V}}(x,t)$ being not always zero except at the origin, then the system is asymptotically stable at the origin;

3) $\boldsymbol{V}(x, t)$ is positive definite, and $\dot{\boldsymbol{V}}(x,t)$ is negative semidefinite, with $\boldsymbol{V}(x, t)\to\infty$ when $\|x\|\to\infty$, then the system is globally asymptotically stable at the origin.

Lemma 1 [18]: A positive scalar function $V(x, t)$ is defined. If

$$\dot{V}(x) + \lambda V^{\theta}(x) \leqslant 0 \tag{2}$$

is satisfied, where $\lambda > 0$ and $0 < \theta < 1$, then the system in Eq. (1) is stable within a finite time, and its finite time T satisfies the following inequality:

$$T \leqslant \frac{1}{\lambda(1-\theta)}[V(x(t_0))]^{1-\theta} \tag{3}$$

where $V(x(t_0))$ is the initial value of $V(x(t))$.

Lemma 2 [19]: In terms of the following system

$$\begin{cases} \dot{\xi}_0 = -\beta_0 L^{\frac{1}{n+1}}|\xi_0|^{\frac{n}{n+1}}\operatorname{sign}(\xi_0) + \xi_1 \\ \dot{\xi}_1 = -\beta_1 L^{\frac{1}{n}}\left|\xi_1 - \dot{\xi}_0\right|^{\frac{n-1}{n}}\operatorname{sign}\left(\xi_1 - \dot{\xi}_0\right) + \xi_2 \\ \quad\vdots \\ \dot{\xi}_{n-1} = -\beta_{n-1} L^{\frac{1}{2}}\left|\xi_{n-1} - \dot{\xi}_{n-2}\right|^{\frac{1}{2}}\operatorname{sign}\left(\xi_{n-1} - \dot{\xi}_{n-2}\right) + \xi_n \\ \dot{\xi}_n \in -\beta_n L\operatorname{sign}\left(\xi_n - \dot{\xi}_{n-1}\right) + [-L, L] \end{cases} \tag{4}$$

where $\beta_i > 0$ ($I = 0, 1, \ldots, n$); L is greater than zero and is a constant; n is the system order. If the system satisfies these conditions, it is stable within a finite time.

1.2 Mathematical model

The motion state of a UUV needs to be described based on a coordinate system. As shown in Fig. 1, the inertial coordinate system E-$\xi\eta\zeta$ is established with the earth as the origin, and the appendage coordinate system O-$x_o y_o z_o$ is established with the gravity center of the UUV as the origin.

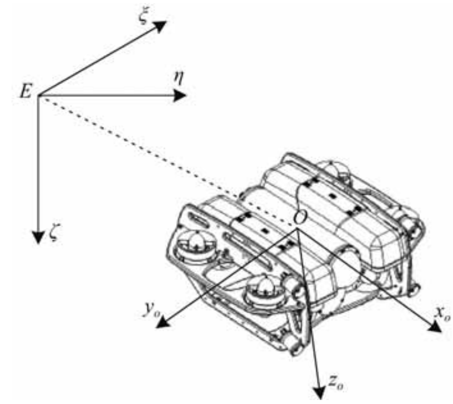

Fig. 1 Coordinate system

According to the submersible dynamic modeling method proposed by Fossen et al. [20], a six-degree-of-freedom mathematical model of the UUV is obtained. Due to the small change in the roll angle of the UUV during the motion, its influence on the UUV can be ignored, and a five-degree-of-freedom mathematical model of the UUV can be obtained.

$$\begin{cases} \dot{\boldsymbol{\eta}} = \boldsymbol{J}(\boldsymbol{\eta})\boldsymbol{\upsilon} \\ \boldsymbol{M}\dot{\boldsymbol{\upsilon}} = \boldsymbol{\tau} + \boldsymbol{\tau}_{\delta} - \boldsymbol{C}(\boldsymbol{\upsilon})\boldsymbol{\upsilon} - \boldsymbol{D}(\boldsymbol{\upsilon})\boldsymbol{\upsilon} - \boldsymbol{g}(\boldsymbol{\eta}) \end{cases} \tag{5}$$

where $\boldsymbol{\eta} = [x, y, z, \theta, \psi]^{\mathrm{T}}$ in the inertial coordinate system; x is the longitudinal displacement of the UUV; y is the lateral displacement; z is the vertical displacement; θ is the pitch angle; ψ is the yaw angle; $\boldsymbol{\upsilon}$ equals $[u, v, w, q, r]^{\mathrm{T}}$ in the appendage coordinate system; u is the longitudinal velocity; v is the lateral velocity; w is the vertical velocity; q is the pitch angular velocity; r is yaw angular velocity; $\boldsymbol{\tau} = [\tau_1, \tau_2, \tau_3, \tau_4, \tau_5]^{\mathrm{T}}$; τ_1 is the longitudinal control force; τ_2 is the lateral control force; τ_3 is the vertical control force; τ_4 is the pitch angle control moment; τ_5 is the yaw angle control moment; $\tau_{\delta} = \boldsymbol{M}\boldsymbol{J}^{-1}(\boldsymbol{\eta})\boldsymbol{\delta}(t)$ is the external interference in the corresponding direction; $\boldsymbol{\delta}(t) = [\delta_1, \delta_2, \delta_3, \delta_4, \delta_5]^{\mathrm{T}}$; $\boldsymbol{M}$ is the mass and additional mass matrix, with $\boldsymbol{M} = \boldsymbol{M}^{\mathrm{T}} > 0$; $\boldsymbol{C}(\boldsymbol{\upsilon})$ is the Coriolis centripetal force matrix, with $\boldsymbol{C}(\boldsymbol{\upsilon}) = -\boldsymbol{C}^{\mathrm{T}}(\boldsymbol{\upsilon})$; $\boldsymbol{D}(\boldsymbol{\upsilon})$ is the damping matrix; $\boldsymbol{g}(\boldsymbol{\eta})$ is the restoring force matrix; $\boldsymbol{J}(\boldsymbol{\eta})$ is the transformation matrix between the inertial coordinate system and the appendage coordinate system, which is described as follows:

$$\boldsymbol{M} = \operatorname{diag}\left(m - X_{\dot{u}}, m - Y_{\dot{v}}, m - Z_{\dot{w}}, I_y - M_{\dot{q}}, I_z - N_{\dot{r}}\right) \tag{6}$$

$$\boldsymbol{C}(\boldsymbol{\upsilon}) = \begin{bmatrix} 0 & 0 & 0 & (m - Z_{\dot{w}})w & -(m - Y_{\dot{v}})v \\ 0 & 0 & 0 & 0 & (m - X_{\dot{u}})u \\ 0 & 0 & 0 & -(m - X_{\dot{u}})u & 0 \\ -(m - Z_{\dot{w}})w & 0 & (m - X_{\dot{u}})u & 0 & 0 \\ (m - Y_{\dot{v}})v & -(m - X_{\dot{u}})u & 0 & 0 & 0 \end{bmatrix} \tag{7}$$

$$\boldsymbol{D}(\boldsymbol{\upsilon}) = -\mathrm{diag}(X_u + X_{u|u|}|u|, Y_v + Y_{v|v|}|v|, Z_w + Z_{w|w|}|w|, M_q + M_{q|q|}|q|, N_r + N_{r|r|}|r|) \tag{8}$$

$$\boldsymbol{g}(\boldsymbol{\eta}) = [(W-B)\sin\theta, 0, -(W-B)\cos\theta, -z_B B\sin\theta, 0]^{\mathrm{T}} \tag{9}$$

$$\boldsymbol{J}(\boldsymbol{\eta}) = \begin{bmatrix} \cos\psi\cos\theta & -\sin\psi & \cos\psi\sin\theta & 0 & 0 \\ \sin\psi\cos\theta & \cos\psi & \sin\psi\sin\theta & 0 & 0 \\ -\sin\theta & 0 & \cos\theta & 0 & 0 \\ 0 & 0 & 0 & 1 & 0 \\ 0 & 0 & 0 & 0 & \sec\theta \end{bmatrix} \tag{10}$$

where m is the mass of the UUV; I_y and I_z are the moments of inertia; $X_{\dot{u}}$, $Y_{\dot{v}}$, $Z_{\dot{w}}$, $M_{\dot{q}}$, $N_{\dot{r}}$ are the hydrodynamic derivatives in the five degrees of freedom (lateral direction, longitudinal direction, vertical direction, pitch angle, and heading angle), respectively; X_u, Y_v, Z_w, M_q, and N_r are the first-order damping coefficients of the five degrees of freedom, respectively. $X_{u|u|}$, $Y_{v|v|}$, $Z_{w|w|}$, $M_{q|q|}$, and $N_{r|r|}$ are the second-order damping coefficients of the five degrees of freedom; W and B are the gravity and buoyancy of the UUV, respectively; z_B is the position the floating center of the appendage coordinate system in the z axis, namely, the height of the floating center.

Control objective: According to the mathematical model of the UUV, i. e. Eq. (5), the mathematical model of the desired trajectory is established, and the tracking error equation is constructed. The controller $\boldsymbol{\tau}$ is then designed based on the equation. When there are a variety of complex external time-varying disturbances, the trajectory tracking system of the UUV based on this control strategy can not only achieve accurate tracking of the desired trajectory within a finite time but also obtain a smooth control input curve.

2 Design of FDO-NTSMC controller

2.1 Problem description

The mathematical model of the desired trajectory is described as follows.

$$\begin{cases} \dot{\boldsymbol{\eta}}_{\mathrm{d}} = \boldsymbol{J}(\boldsymbol{\eta}_{\mathrm{d}})\boldsymbol{\upsilon}_{\mathrm{d}} \\ \boldsymbol{M}\dot{\boldsymbol{\upsilon}}_{\mathrm{d}} = \tau_{\mathrm{d}} - \boldsymbol{C}(\boldsymbol{\upsilon}_{\mathrm{d}})\boldsymbol{\upsilon}_{\mathrm{d}} - \boldsymbol{D}(\boldsymbol{\upsilon}_{\mathrm{d}})\boldsymbol{\upsilon}_{\mathrm{d}} - \boldsymbol{g}(\eta_{\mathrm{d}}) \end{cases} \tag{11}$$

where $\boldsymbol{\eta}_{\mathrm{d}}$ equals $[x_{\mathrm{d}}, y_{\mathrm{d}}, z_{\mathrm{d}}, \theta_{\mathrm{d}}, \psi_{\mathrm{d}}]^{\mathrm{T}}$, and it is the desired position and heading angle; $\boldsymbol{\upsilon}_{\mathrm{d}}$ equals $[u_{\mathrm{d}}, v_{\mathrm{d}}, w_{\mathrm{d}}, q_{\mathrm{d}}, r_{\mathrm{d}}]^{\mathrm{T}}$, and it is the desired velocity and angular velocity; $\boldsymbol{\tau}_{\mathrm{d}}$ equals $[\tau_{\mathrm{d1}}, \tau_{\mathrm{d2}}, \tau_{\mathrm{d3}}, \tau_{\mathrm{d4}}, \tau_{\mathrm{d5}}]^{\mathrm{T}}$, and it is the control input corresponding to the desired trajectory.

In order to facilitate the description of the controller's design process, the following state variables are defined:

$$\begin{cases} \omega = \boldsymbol{J}(\boldsymbol{\eta})\boldsymbol{\upsilon} \\ \omega_{\mathrm{d}} = \boldsymbol{J}(\boldsymbol{\eta}_{\mathrm{d}})\boldsymbol{\upsilon}_{\mathrm{d}} \end{cases} \tag{12}$$

where $\boldsymbol{\omega}$ equals $[\omega_1, \omega_2, \omega_3, \omega_4, \omega_5]^{\mathrm{T}}$, and it is the actual desired position and heading angle; $\boldsymbol{\omega}_{\mathrm{d}}$ equals $[\omega_{\mathrm{d1}}, \omega_{\mathrm{d2}}, \omega_{\mathrm{d3}}, \omega_{\mathrm{d4}}, \omega_{\mathrm{d5}}]^{\mathrm{T}}$, and it is the actual velocity and angular velocity; ω_1−ω_5 are the actual values of longitudinal, lateral, and vertical velocities, as well as angular velocities of pitch angle and heading angle of the UUV in the inertial coordinate system; ω_{d1}−ω_{d5} are the desired values corresponding to the above five variables.

Combined with the state variable equation, Eq. (5) is rewritten as

$$\begin{cases} \dot{\boldsymbol{\eta}} = \boldsymbol{\omega} \\ \dot{\omega} = \boldsymbol{J}(\boldsymbol{\eta})\boldsymbol{M}^{-1}\tau + \boldsymbol{\delta} + \boldsymbol{\Theta} \end{cases} \tag{13}$$

where

$$\boldsymbol{\Theta} = -\boldsymbol{J}(\boldsymbol{\eta})\boldsymbol{M}^{-1}(\boldsymbol{C}(\boldsymbol{\upsilon}) + \boldsymbol{D}(\boldsymbol{\upsilon}))J(\boldsymbol{\eta})^{-1}\boldsymbol{\omega} - \boldsymbol{J}(\boldsymbol{\eta})\dot{J}(\boldsymbol{\eta})^{-1}\boldsymbol{\omega} - \boldsymbol{J}(\boldsymbol{\eta})\boldsymbol{M}^{-1}\boldsymbol{g}(\boldsymbol{\eta})$$

Similarly, Eq.(11) can be rewritten as

$$\begin{cases} \dot{\boldsymbol{\eta}}_{\mathrm{d}} = \boldsymbol{\omega}_{\mathrm{d}} \\ \dot{\omega}_{\mathrm{d}} = \boldsymbol{J}(\boldsymbol{\eta}_{\mathrm{d}})\boldsymbol{M}^{-1}\boldsymbol{\tau}_{\mathrm{d}} + \boldsymbol{\Theta}_{\mathrm{d}} \end{cases} \tag{14}$$

where

$$\boldsymbol{\Theta}_{\mathrm{d}} = -\boldsymbol{J}(\boldsymbol{\eta}_{\mathrm{d}})\boldsymbol{M}^{-1}(\boldsymbol{C}(\boldsymbol{\upsilon}_{\mathrm{d}}) + \boldsymbol{D}(\boldsymbol{\upsilon}_{\mathrm{d}}))J(\boldsymbol{\eta}_{\mathrm{d}})^{-1}\boldsymbol{\omega}_{\mathrm{d}} - \boldsymbol{J}(\boldsymbol{\eta}_{\mathrm{d}})\dot{J}(\boldsymbol{\eta}_{\mathrm{d}})^{-1}\omega_{\mathrm{d}} - \boldsymbol{J}(\boldsymbol{\eta}_{\mathrm{d}})\boldsymbol{M}^{-1}\boldsymbol{g}(\boldsymbol{\eta}_{\mathrm{d}})$$

By combining Eq. (13) and Eq. (14), this paper obtains the tracking error equation of the system:

$$\begin{cases} \dot{\boldsymbol{\eta}}_{\mathrm{e}} = \boldsymbol{\omega}_{\mathrm{e}} \\ \dot{\omega}_{\mathrm{e}} = \boldsymbol{J}(\boldsymbol{\eta}_{\mathrm{e}})\boldsymbol{M}^{-1}\tau + \boldsymbol{\delta} + \boldsymbol{\Theta}_{\mathrm{e}} \end{cases} \tag{15}$$

where

$$\boldsymbol{\Theta}_{\mathrm{e}} = -\boldsymbol{J}(\boldsymbol{\eta}_{\mathrm{d}})\boldsymbol{M}^{-1}\tau_{\mathrm{d}} + \boldsymbol{\Theta} - \boldsymbol{\Theta}_{\mathrm{d}}$$
$$\boldsymbol{\omega}_{\mathrm{e}} = [\omega_{\mathrm{e1}}, \omega_{\mathrm{e2}}, \omega_{\mathrm{e3}}, \omega_{\mathrm{e4}}, \omega_{\mathrm{e5}}]^{\mathrm{T}}$$

2.2 Design of controller

Under the multidimensional external disturbances, the FDO-NTSMC controller is designed based on Eq. (15) to realize the accurate tracking of the 3D desired trajectory of the UUV.

Step 1: A FDO is designed to compensate for the multi-dimensional external time-varying disturbances.

Assumption 1: External disturbance $\boldsymbol{\delta}$ in Eq. (15) satisfies

$$\|\ddot{\delta}\| \leqslant L_\delta \tag{16}$$

where L_δ is a constant, and it is greater than zero and bounded.

For the disturbances in the tracking error system equation, the FDO is designed as follows:

$$\begin{cases} \dot{z}_0 = \xi_0 + \boldsymbol{J}(\boldsymbol{\eta})\boldsymbol{M}^{-1}\boldsymbol{\tau} + \boldsymbol{\Theta}_{\mathrm{e}} \\ \dot{z}_1 = \xi_1 \\ \dot{z}_2 = \xi_2 \end{cases} \tag{17}$$

where

$$\begin{cases}\xi_0 = -\beta_1 L^{1/3}\mathrm{sig}^{2/3}(z_0-\omega_\mathrm{e})+z_1 \\ \xi_1 = -\beta_2 L^{1/2}\mathrm{sig}^{1/2}(z_1-\xi_0)+z_2 \\ \xi_2 = -\beta_3 L\,\mathrm{sign}(z_2-\xi_1)\end{cases} \tag{18}$$

where z_0 is the estimated value of the velocity error; z_1 is the observed value of external disturbances; z_2 is the estimated value of the first-order derivative of external disturbances; $z_\mathrm{i} \in \mathrm{R}^{5\times1}$ $(i=0,1,2)$; β_i is greater than 0 (i = 0, 1, 2) and is the gain coefficient; $\boldsymbol{L}$ equals diag (l_1, l_2, l_3, l_4, l_5) and is the parameter of the FDO; $\mathrm{sig}^\theta(x)$ equals $|x|^\theta\,\mathrm{sign}(x)$.

Step 2: Design the nonsingular terminal sliding mode surface $\boldsymbol{s}$:

$$\boldsymbol{s} = \boldsymbol{\eta}_\mathrm{e} + k\boldsymbol{\omega}_\mathrm{e}^{q/p} \tag{19}$$

where k is greater than zero and is a constant; p and q are positive odd numbers, and $q/p \in (1,2)$.

By taking the derivation of Eq. (19) and combining Eq. (15), this paper can obtain

$$\dot{s} = \omega_\mathrm{e} + \frac{qk}{p}\mathrm{diag}\left(\omega_\mathrm{e}^{q/p-1}\right)\left(\boldsymbol{J}(\boldsymbol{\eta})\boldsymbol{M}^{-1}\boldsymbol{\tau}+\boldsymbol{\delta}+\boldsymbol{\Theta}_\mathrm{e}\right) \tag{20}$$

where diag(·) represents the diagonal matrix. To ensure the correct dimension after the derivation, the paper rewrites $\boldsymbol{\omega}_\mathrm{e}^{q/p-1}$ as diag($\boldsymbol{\omega}_\mathrm{e}^{q/p-1}$).

According to Eq. (20), the controller can be designed as

$$\boldsymbol{\tau} = \boldsymbol{\tau}_\mathrm{eq} + \boldsymbol{\tau}_\mathrm{s} \tag{21}$$

where the equivalent control term is

$$\boldsymbol{\tau}_\mathrm{eq} = -\boldsymbol{M}\boldsymbol{J}^{-1}(\boldsymbol{\eta})\left(\frac{p}{qk}\omega_\mathrm{e}^{2-q/p}+z_1+\boldsymbol{\Theta}_\mathrm{e}\right) \tag{22}$$

and the robust control term is

$$\boldsymbol{\tau}_\mathrm{s} = -\boldsymbol{M}\boldsymbol{J}^{-1}(\boldsymbol{\eta})\boldsymbol{\kappa}|\boldsymbol{s}|^\alpha\mathrm{sign}(\boldsymbol{s}) \tag{23}$$

In the equation, the power reaching law $\dot{s} = \boldsymbol{\kappa}|\boldsymbol{s}|^\alpha\mathrm{sign}(\boldsymbol{s})$ is selected to ensure that the sliding surface is reached within a finite time. Specifically, $\boldsymbol{\kappa}$ equals diag(κ_1, κ_2, κ_3, κ_4, κ_5); κ_i is greater than zero (i = 1, 2, 3, 4, 5) and is a constant diagonal matrix; α is a constant, and $0 < \alpha < 1$; sign($\boldsymbol{s}$) = [sign(s_1), sign(s_2), sign(s_3), sign(s_4), sign(s_5)]$^\mathrm{T}$; sign(·) denotes the sign function and has the following properties:

$$\mathrm{sign}(x) = \begin{cases} 1, & x>0 \\ 0, & x=0 \\ -1, & x<0\end{cases} \tag{24}$$

2.3 System stability analysis

Theorem 2: For the multi-dimensional complex time-varying disturbances in Assumption 1, the designed FDO can observe the disturbance and compensate for the influence of the disturbance on the system to improve the robustness.

Proof:

For the designed FDO in Eq. (17), the observation error equation is defined as

$$\begin{cases}\boldsymbol{e}_0 = z_0 - \boldsymbol{\omega}_\mathrm{e} \\ \boldsymbol{e}_1 = z_1 - \boldsymbol{\delta} \\ \boldsymbol{e}_2 = z_2 - \dot{\boldsymbol{\delta}}\end{cases} \tag{25}$$

By taking the derivation at both ends of the equation and combining Eq. (17) with Eq. (18), there is

$$\begin{cases}\dot{\boldsymbol{e}}_0 = -\beta_1\boldsymbol{L}^{1/3}\mathrm{sig}^{2/3}(\boldsymbol{e}_0)+\boldsymbol{e}_1 \\ \dot{\boldsymbol{e}}_1 = -\beta_2\boldsymbol{L}^{1/2}\mathrm{sig}^{1/2}(\boldsymbol{e}_1-\dot{\boldsymbol{e}}_0)+\boldsymbol{e}_2 \\ \dot{\boldsymbol{e}}_2 = -\beta_3\boldsymbol{L}\mathrm{sign}(\boldsymbol{e}_2-\dot{\boldsymbol{e}}_1)-\ddot{\boldsymbol{\delta}}\end{cases} \tag{26}$$

Eq. (26) can also be rewritten as

$$\begin{cases}\dot{e}_{i0} = -\beta_1 L_i^{1/3}\mathrm{sig}^{2/3}(e_{i0})+e_{i1} \\ \dot{e}_{i1} = -\beta_2 L_i^{1/2}\mathrm{sig}^{1/2}(e_{i1}-\dot{e}_{i0})+e_{i2} \\ \dot{e}_{i2} = -\beta_3 L_i\mathrm{sign}(e_{i2}-\dot{e}_{i1})+[-L_\delta, L_\delta]\end{cases} \tag{27}$$

Lemma 2 shows that Eq. (27) is stable within a finite time. In other words, the designed FDO can observe the disturbance within a finite time. Besides, within the finite time, there is

$$\begin{cases} z_0 \equiv \boldsymbol{\omega}_\mathrm{e} \\ z_1 \equiv \boldsymbol{\delta} \\ z_2 \equiv \dot{\boldsymbol{\delta}}\end{cases} \tag{28}$$

Therefore, the observation error $\boldsymbol{z}_1 - \boldsymbol{\delta} \equiv 0$ can be obtained. QED.

Theorem 3: In view of the mathematical model of the UUV under the influence of multi-dimensional external time-varying disturbances $\boldsymbol{\delta}$, the system can drive state variables to reach the sliding surface $\boldsymbol{s}(t)$ = 0 within a finite time under the action of control law $\boldsymbol{\tau}$, so that the pose tracking error variable can converge to zero within a finite time. In other words, the tracking of actual pose vector $\boldsymbol{\eta}$ and velocity vector $\boldsymbol{\upsilon}$ learns from pose vector $\boldsymbol{\eta}_\mathrm{d}$ and the desired velocity vector $\boldsymbol{\upsilon}_\mathrm{d}$.

Proof:

By substituting Eq. (21) into Eq. (20), this paper gets

$$\dot{\boldsymbol{s}} = -\frac{qk}{p}\mathrm{diag}\left(\omega_\mathrm{e}^{q/p-1}\right)\left(z_1-\boldsymbol{\delta}+\boldsymbol{\kappa}|\boldsymbol{s}|^\alpha\mathrm{sign}(\boldsymbol{s})\right) \tag{29}$$

Based on Theorem 1, the above equation can be written as

$$\dot{\boldsymbol{s}} = -\frac{qk}{p}\mathrm{diag}\left(\omega_\mathrm{e}^{q/p-1}\right)\boldsymbol{\kappa}|\boldsymbol{s}|^\alpha\mathrm{sign}(\boldsymbol{s}) \tag{30}$$

The Lyapunov function is defined as

$$V = \frac{1}{2}\boldsymbol{s}^\mathrm{T}\boldsymbol{s} \tag{31}$$

By taking the derivation of the equation and substituting it into Eq. (30), the paper gets

$$\dot{V} = \boldsymbol{s}^\mathrm{T}\dot{\boldsymbol{s}} = -\boldsymbol{s}^\mathrm{T}\left(\frac{qk}{p}\mathrm{diag}\left(\omega_\mathrm{e}^{q/p-1}\right)\boldsymbol{\kappa}|\boldsymbol{s}|^\alpha\mathrm{sign}(\boldsymbol{s})\right) \tag{32}$$

Let

$$\boldsymbol{Q} = \frac{qk}{p}\mathrm{diag}\left(\omega_\mathrm{e}^{q/p-1}\right)\boldsymbol{\kappa} \tag{33}$$

When $\omega_{\mathrm{e}i} \neq 0$ (i = 1, 2, 3, 4, 5), since $q/p-1 > 0$, $k > 0$, and $\boldsymbol{\kappa} > 0$, with q and p being positive odd numbers, the paper can get a positive definite matrix $\boldsymbol{Q}$, that is, $\lambda_{\min}(\boldsymbol{Q}) \geqslant 0$. Then, Eq. (32) can be rewritten as

$$\dot{V} \leqslant -\lambda_{\min}(\boldsymbol{Q}) \sum_{i=1}^{5} |s_i|^{\alpha+1} \tag{34}$$

According to Theorem 1, the system is asymptotically stable. The following steps further prove the finite-time stability of the system. Let

$$\rho = 2^{(\alpha+1)/2} \lambda_{\min}(\boldsymbol{Q}) \tag{35}$$

By combining Eq. (31) with Eq. (34) and Eq. (35), the paper gets

$$\dot{V} \leqslant -\rho V^{(\alpha+1)/2} \tag{36}$$

where $0 < \alpha < 1$ and $1/2 < (\alpha + 1)/2 < 1$. According to Lemma 1, the system converges within a finite time.

When $\omega_{ei} \neq 0$ (i = 1, 2, 3, 4, 5), according to Eqs. (21)−(23) and Eq. (15), the following equation is obtained:

$$\omega_{\mathrm{e}} = -\boldsymbol{\kappa} |\boldsymbol{s}|^{\alpha} \mathrm{sign}(\boldsymbol{s}) \tag{37}$$

From the above equation, when $s_i > 0$, $\dot{\omega}_{ei} < 0$, and ω_{ei} decreases rapidly. When $s_i < 0$, $\dot{\omega}_{ei} > 0$, and ω_{ei} increases rapidly. Therefore, when ω_{ei} equals zero, $\boldsymbol{s}(t)$ equals zero within a finite time. In other words, the tracking error $\boldsymbol{\eta}_{\mathrm{e}}$ and the velocity tracking error $\boldsymbol{\omega}_{\mathrm{e}}$ reach the sliding mode surface within a finite time [21].

According to the above proof, the proposed FDO-NTSMC can make the UUV achieve accurate 3D trajectory tracking within a finite time, and the tracking error of the system can converge to zero within a finite time.

3 Simulation experiment study

In order to prove the superiority and effectiveness of the designed controller, the dynamic model and hydrodynamic parameters of the UUV in Ref. [22] were used, and the simulation experiment in which the BSMC and NTSMC are compared was carried out under the same initial conditions. At the same time, to verify the transient and steady-state accuracy based on the proposed method, the integral absolute error (IAE) and the integral time absolute error (ITAE) were used for measurement [23-24]. The expression is as follows.

$$f_{\mathrm{IAE}} = \int_0^t |e(\boldsymbol{\tau})| \mathrm{d}\tau \tag{38}$$

$$f_{\mathrm{ITAE}} = \int_0^t t|e(\boldsymbol{\tau})| \mathrm{d}\tau \tag{39}$$

where $e(\cdot)$ represents the pose tracking error. The result calculated by IAE is f_{IAE}, and that by ITAE is f_{ITAE}.

Specifically, the control input that can generate the desired trajectory $\boldsymbol{\tau}_{\mathrm{d}}$ equals [50, 30cos(0.1πt)^2, 20cos(0.1π t)^2, −12cos(0.1π t)^2, 12cos(0.1π t)^2]$^{\mathrm{T}}$. The initial pose of the UUV $\boldsymbol{\eta}(0)$ equals [15, 7.2, 2.7, 0, 0]$^{\mathrm{T}}$, and the initial velocity and angular velocity $\boldsymbol{\upsilon}(0)$ equal [0, 0, 0, 0, 0]$^{\mathrm{T}}$. Here, $\boldsymbol{\delta}$ equals [0.3cos(0.2π t−π/3), 0.4cos(0.4π t−π/4), 0.6cos(0.6π t−π/6), 0.2cos(0.2π t − π/2), 0.3cos(0.4π t− π/3)]$^{\mathrm{T}}$, and the step disturbance δ_2 equals [5, 5, 5, 5, 5]$^{\mathrm{T}}$. The key parameters of the FDO-NTSMC controller are as follows: q = 7; p = 5; k = 2; α = 0.7; $\boldsymbol{\kappa}$ = diag(3.6, 3.6, 3.6, 3.6, 3.6). The parameters of the FDO are as follows: β_1 = 2.2; β_2 = 2.6; β_3 = 0.8; L = diag(30, 30, 30, 30, 30).

1) Simulation experiment condition 1: When there was an underwater disturbance $\boldsymbol{\delta}$, simulation experiments of the 3D trajectory tracking of the UUV were carried out based on the proposed algorithm and NTSMC and BSMC algorithms, respectively. The simulation results are shown in Figs. 2-8.

From Figs. 2-4, it can be seen that when there was an underwater disturbance $\boldsymbol{\delta}$, although the

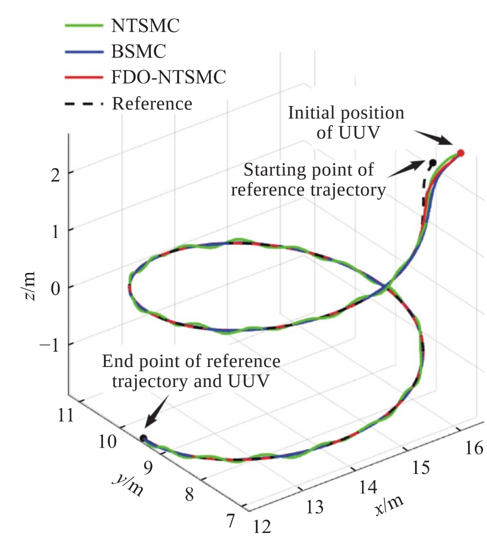

Fig. 2 Tracking trajectory under condition 1

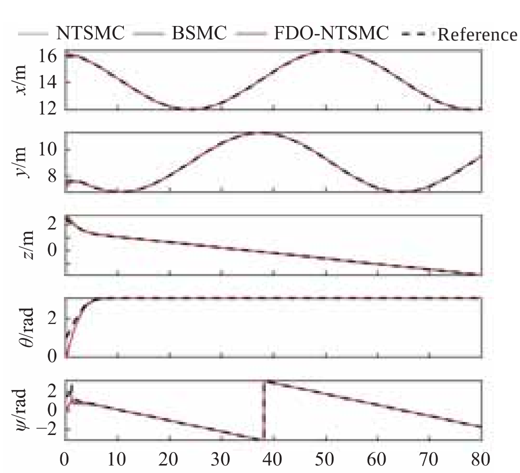

Fig. 3 Pose states under condition 1

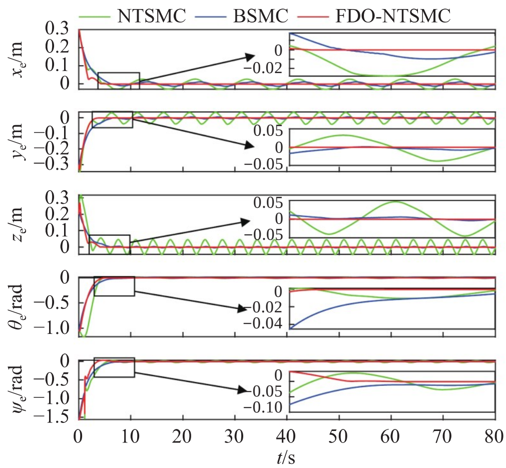

Fig. 4 Pose tracking errors under condition 1

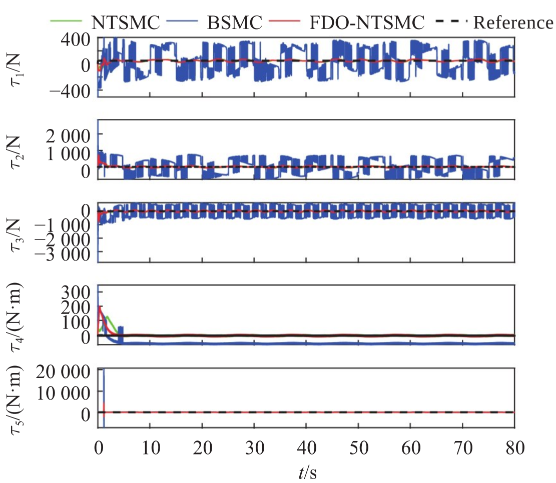

Fig. 5 Control input under condition 1

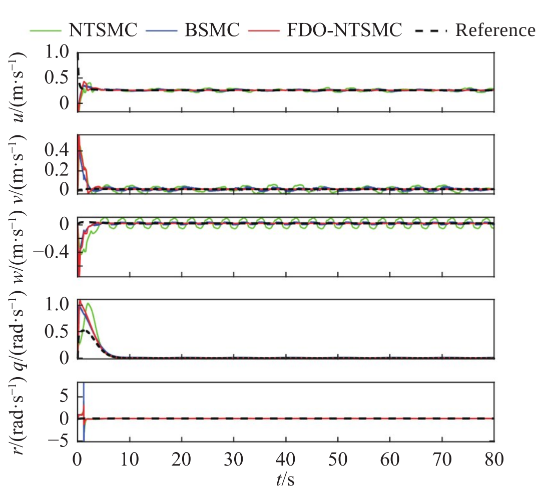

Fig. 6 Velocity states under condition 1

NTSMC and BSMC control strategies can make the UUV track the desired trajectory, they cannot achieve accurate tracking. In other words, there is a fluctuating tracking error. However, the FDO-NTSMC control strategy can make the trajectory tracking error stay at zero. The control input curve in Fig. 5 shows that compared with the BSMC strategy, the FDO-NTSMC can realize a smoother con-

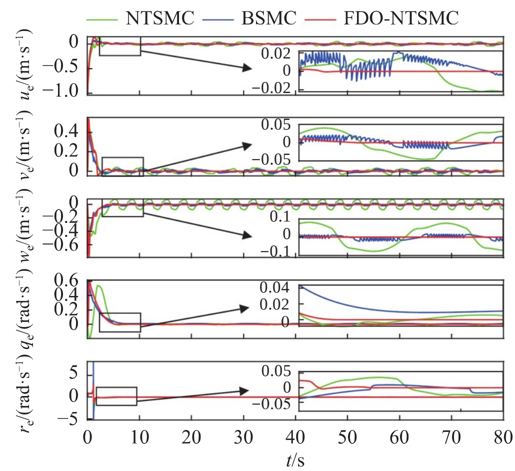

Fig. 7 Velocity tracking errors under condition 1

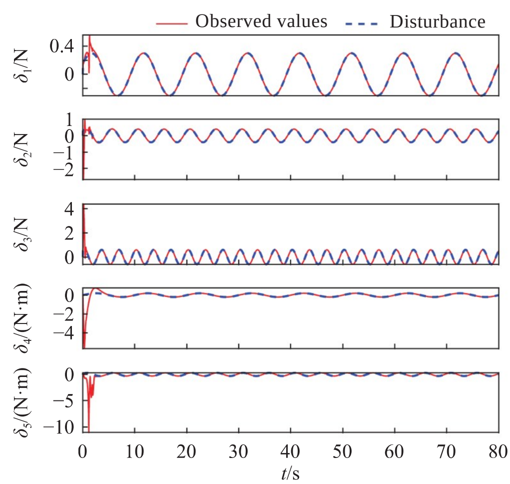

Fig. 8 Underwater disturbance and observed values under condition 1

trol input, which can facilitate the operation of the actuator, and its FDO can accurately observe the complex external disturbances (Fig. 8). As a result, it can compensate for the interference of external disturbances on the system in time and improve the anti-jamming ability of the system. The velocity and velocity error curves in Fig. 6 and Fig. 7 show that the designed controller has better performance than NTSMC.

2) Simulation experiment condition 2: In addition to $\boldsymbol{\delta}$ in the underwater environment, a step disturbance was added at 30−40 s. Under the same initial conditions, the simulation results of FDO-NTSMC, NTSMC, and BSMC were obtained, as shown in Figs. 9-15.

It can be seen from Fig. 9 that after the step disturbance is added at 30−40 s, the NTSMC and BSMC control strategies cannot track the reference trajectory, while the proposed FDO-NTSMC can still accurately track the reference trajectory, which is also verified by the pose tracking error results in

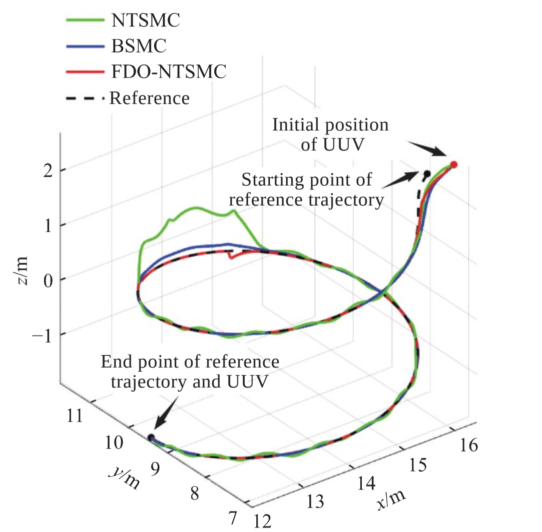

Fig. 9 Tracking trajectory under condition 2

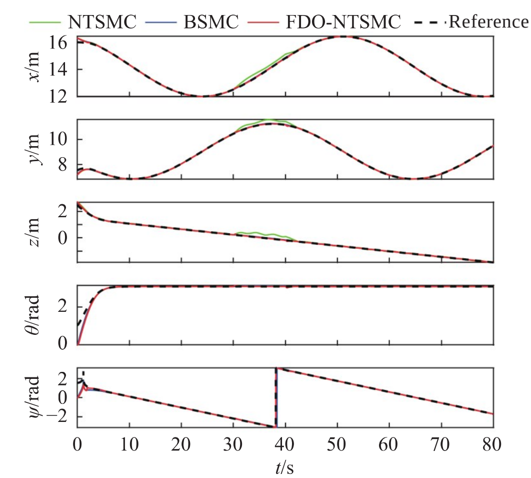

Fig. 10 Pose states under condition 2

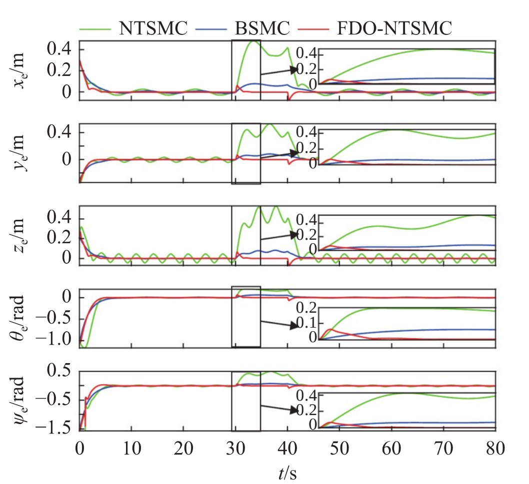

Fig. 11 Pose tracking errors under condition 2

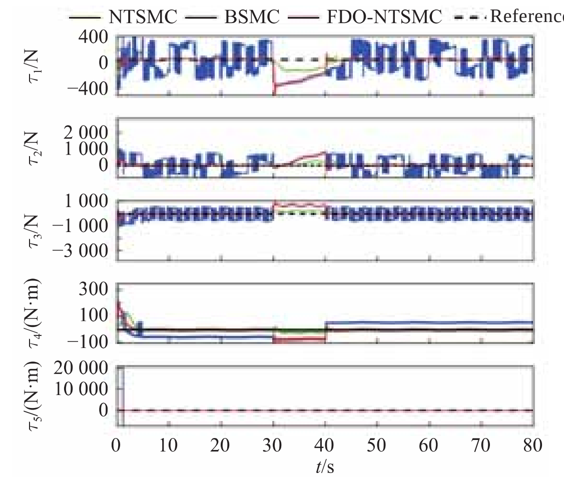

Fig. 12 Control input under condition 2

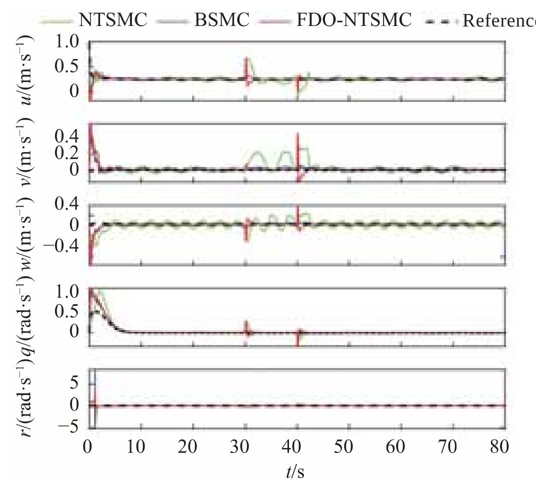

Fig. 13 Velocity states under condition 2

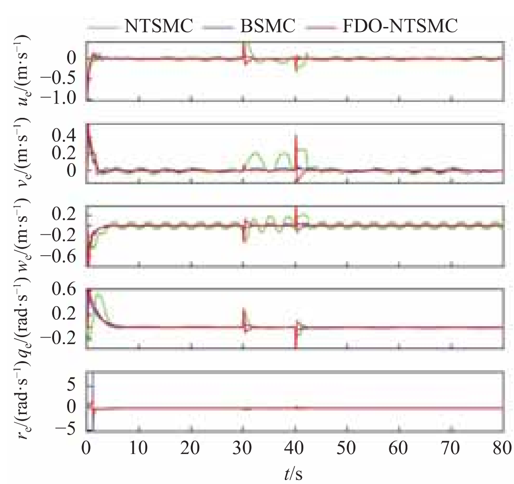

Fig. 14 Velocity tracking errors under condition 2

Fig. 11. It can be seen from Fig. 15 that, after the step disturbance is added, the designed FDO can still accurately observe the disturbances to compensate for the influence of the step disturbance on the system in time and thus improve the robustness of the trajectory tracking system.

3) Simulation experiment condition 3: According to the control input curves under condition 1, due to the large trajectory tracking error of the UUV at the initial moment and the multi-dimensional time varying disturbances, great power is needed, which leads to a large step mutation appearing in the curves. However, this does not exist in practical engineering applications, and the actuator needs to work in a safe range, so the amplitudes of the con-

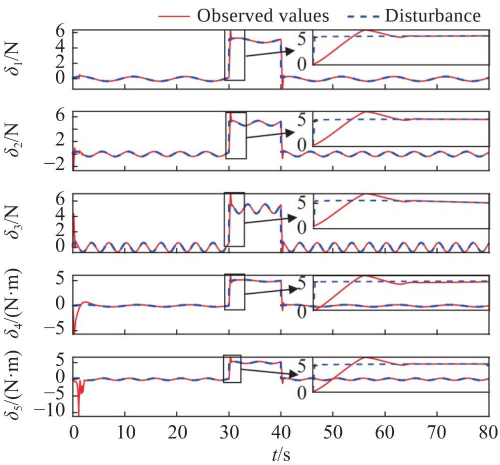

Fig. 15 Underwater disturbance and observed values under condition 2

trol inputs under the three methods should be reasonably limited. As shown in Figs. 16-22, experimental results were obtained.

It can be seen from Fig. 19 that after the amplitude of the controller is limited, strong buffeting appears in the control input curve of BSMC, while

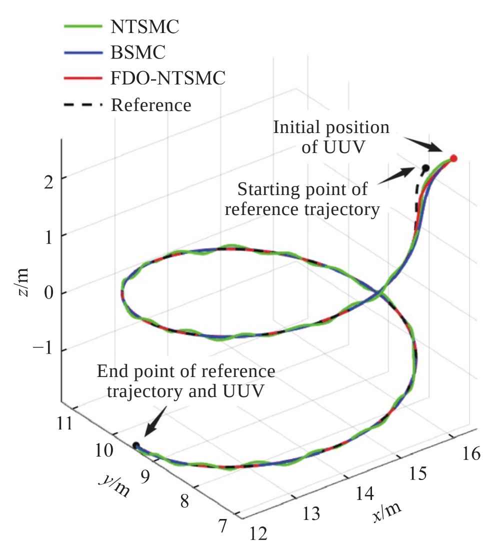

Fig. 16 Tracking trajectory under condition 3

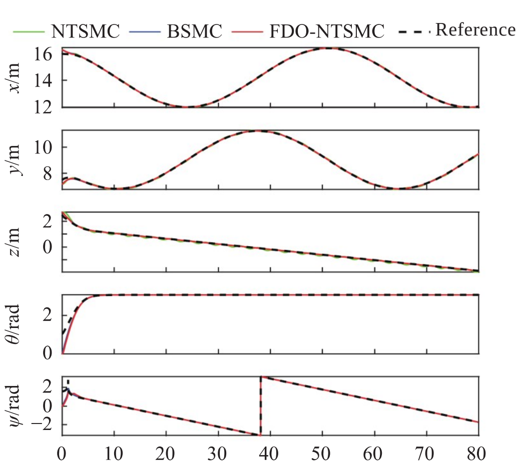

Fig. 17 Pose states under condition 3

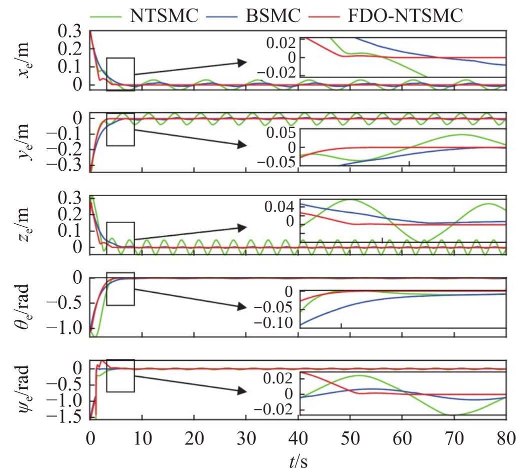

Fig. 18 Pose tracking errors under condition 3

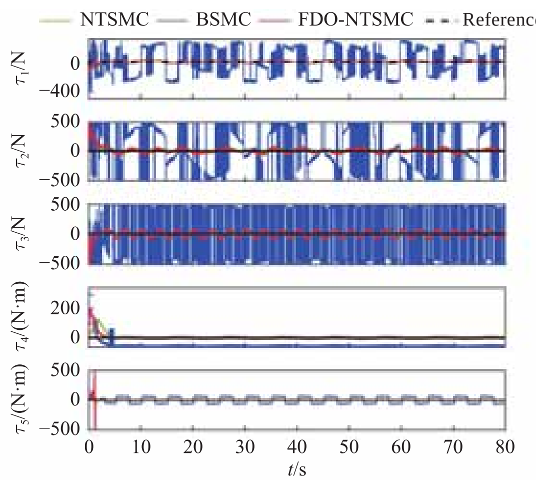

Fig. 19 Control input under condition 3

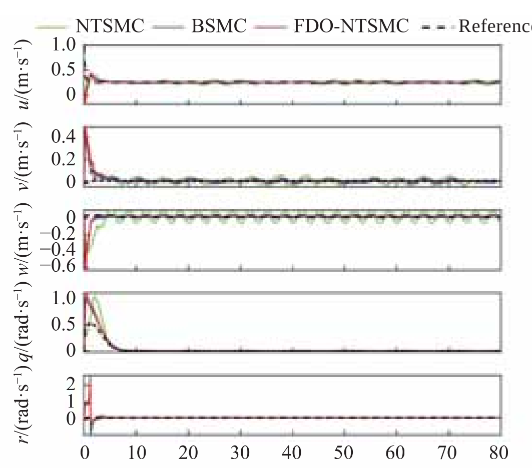

Fig. 20 Velocity states under condition 3

the proposed method obtains a relatively smooth control input curve, which is consistent with that before amplitude limitation. The above contents are the qualitative analysis of the 3D trajectory tracking control of the UUV based on three control methods. In order to more intuitively analyze the advantages of the proposed method, the IAE and the ITAE indexes were used to quantitatively analyze the tran-

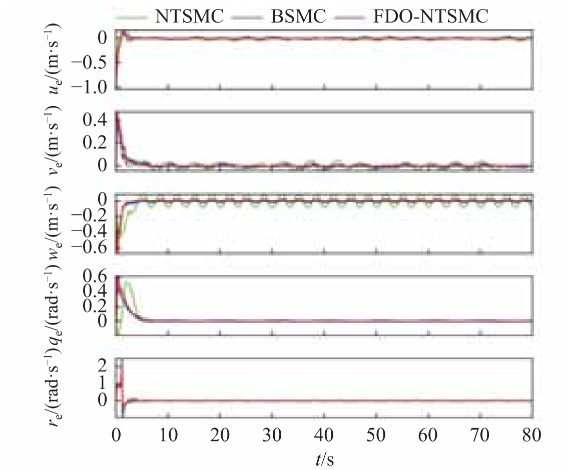

Fig. 21 Velocity tracking errors under condition 3

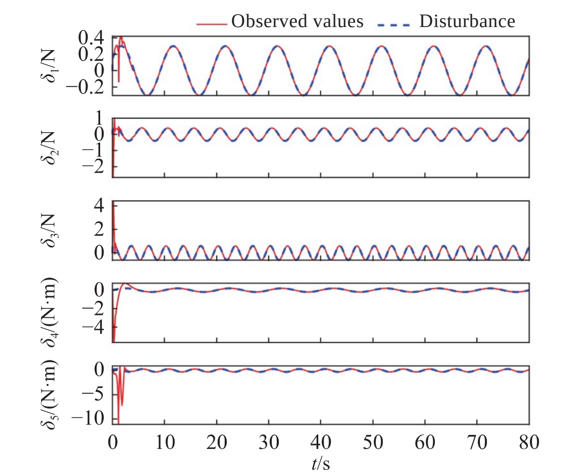

Fig. 22 Underwater disturbance and observed values under condition 3

sient and steady-state accuracy of the control performance under the three conditions. The results are shown in Tables 1–3.

In terms of the IAE indexes under three conditions, the paper finds that BSMC and FDO-NTSMC are smaller than NTSMC, and the proposed FDO-NTSMC method is slightly smaller than BSMC, which indicates a high transient accuracy. Furthermore, the ITAE indexes under three conditions are compared, and the results show that the ITAE performance index of FDO-NTSMC is much lower than that of BSMC and NTSMC. Therefore, the FDO-NTSMC control method can make the UUV achieve high-precision tracking of the desired 3D reference trajectory. In other words, the superiority of the proposed control strategy is further verified quantitatively. The FDO-NTSMC control method has high steady-state accuracy [25].

Table 1 Performance comparison of three methods

Performance index		FDO-NTSMC	BSMC	NTSMC
IAE	x_e	0.462 7	1.061 0	1.265 8
	y_e	0.356 2	0.766 6	1.603 3
	z_e	0.395 6	0.528 4	2.460 3
	θ_e	1.593 2	2.050 1	2.326 6
	ψ_e	2.656 4	2.848 2	4.142 3
ITAE	x_e	0.561 2	24.282 7	33.159 9
	y_e	0.292 6	11.964 8	51.427 9
	z_e	0.460 6	7.384 6	80.571 9
	θ_e	1.779 8	16.042 0	16.232 8
	ψ_e	3.749 6	17.936 6	39.832 9

Table 2 Performance comparison of three methods under step disturbance

Performance index		FDO-NTSMC	BSMC	NTSMC
IAE	x_e	0.626 5	1.718 2	5.916 2
	y_e	0.513 5	1.456 3	6.499 6
	z_e	0.555 3	1.234 4	7.711 7
	θ_e	1.740 6	2.576 4	5.167 5
	ψ_e	2.820 2	3.520 0	8.959 2
ITAE	x_e	6.568 8	48.180 9	203.403 5
	y_e	5.986 0	37.016 3	231.457 9
	z_e	6.288 3	33.114 5	272.619 8
	θ_e	7.129 9	35.028 3	85.621 4
	ψ_e	9.733 6	42.372 9	213.641 1

Table 3 Performance comparison of three methods under amplitude limitation

Performance index		FDO-NTSMC	BSMC	NTSMC
IAE	x_e	0.466 3	0.940 9	1.767 4
	y_e	0.381 3	0.815 4	2.326 4
	z_e	0.437 5	0.641 1	3.513 0
	θ_e	1.593 2	2.050 1	3.422 3
	ψ_e	1.994 5	1.690 2	3.192 1
ITAE	x_e	0.567 2	19.343 2	52.946 8
	y_e	0.322 0	11.429 8	80.644 2
	z_e	0.528 2	7.112 8	119.339 1
	θ_e	1.779 8	16.042 0	23.617 4
	ψ_e	2.423 6	14.800 6	56.396 3

4 Conclusions

In this paper, an FDO-NTSMC control strategy was proposed to accurately track the 3D trajectory of a UUV under complex multi-dimensional time-varying disturbances. An FDO was designed to deal with the underwater complex time-varying disturbances on the trajectory tracking system of the UUV, and theoretical verification was carried out. At the same time, in order to lower the buffeting generated by the NTSMC, the power reaching law was used to replace the constant-speed reaching law used in the previous Ref. [26], which ensured that the tracking error could converge to zero within a finite time. Finally, under the same simulation experiment conditions, the FDO-NTSMC was compared with NTSMC and BSMC control strategies, and the tracking accuracy was quantified by using the IAE and ITAE performance indexes. The simulation results verified the effectiveness and superiority of the proposed strategy.

References

[1] XIANG X B, LAPIERRE L, JOUVENCEL B. Smooth transition of AUV motion control: from fully-actuated to under-actuated configuration [J]. Robotics and Autonomous Systems, 2015, 67: 14−22.

[2] SANTHAKUMAR M, ASOKAN T. Power efficient dynamic station keeping control of a flat-fish type autonomous underwater vehicle through design modifications of thruster configuration [J]. Ocean Engineering, 2013, 58: 11−21.

[3] LI H P, YAN W S. Model predictive stabilization of constrained underactuated autonomous underwater vehicles with guaranteed feasibility and stability [J]. IEEE/ASME Transactions on Mechatronics, 2017, 22 (3): 1185−1194.

[4] SHEN C, SHI Y. Distributed implementation of nonlinear model predictive control for AUV trajectory tracking [J]. Automatica, 2020, 115: 108863.

[5] QIAO L, ZHANG W D. Double-loop integral terminal sliding mode tracking control for UUVs with adaptive dynamic compensation of uncertainties and disturbances [J]. IEEE Journal of Oceanic Engineering, 2019, 44 (1): 29−53.

[6] WANG F, WAN L, LI Y, et al. A survey on development of motion control for underactuated AUV[J]. Shipbuilding of China, 2010, 51 (2): 227−241 (in Chinese).

[7] QIAO L, ZHANG W D. Double-loop chattering-free adaptive integral sliding mode control for underwater vehicles [C]//OCEANS 2016-Shanghai. Shanghai: IEEE, 2016: 1−6.

[8] REZAZADEGAN F, SHOJAEI K, SHEIKHOLESLAMF, et al. A novel approach to 6 - DOF adaptive trajectory tracking control of an AUV in the presence of parameter uncertainties [J]. Ocean Engineering, 2015, 107: 246−258.

[9] GUERRERO J, TORRES J, CREUZE V, et al. Trajectory tracking for autonomous underwater vehicle: an adaptive approach [J]. Ocean Engineering, 2019, 172: 511−522.

[10] QIAO L, ZHANG W D. Adaptive non-singular integral terminal sliding mode tracking control for autonomous underwater vehicles [J]. IET Control Theory & Applications, 2017, 11 (8): 1293−1306.

[11] SUN Q M, CHEN J G, YU W. 3D trajectory-tracking control of autonomous underwater vehicles based on backstepping and sliding mode method [J]. Ship Science and Technology, 2019, 41 (1): 66−70 (in Chinese).

[12] WEI S H, LIU H, MA N, et al. Tracking control for tethered underwater vehicle based on backstepping mode and neurodynamics model [J]. Ship Science and Technology, 2020, 42 (1): 88−94 (in Chinese).

[13] ZHANG W, TENG Y B, WEI S L, et al. Underactuated UUV tracking control of adaptive RBF neural network and backstepping method [J]. Journal of Harbin Engineering University, 2018, 39 (1): 93−99 (in Chinese).

[14] YAN Z P, DUAN H P. A double closed-loop terminal sliding mode controller for the trajectory tracking of UUV [J]. Chinese Journal of Ship Research, 2015, 10 (4): 112−117, 142 (in Chinese).

[15] WANG N, KARIMI H R. Successive waypoints tracking of an underactuated surface vehicle [J]. IEEE Transactions on Industrial Informatics, 2020, 16 (2): 898−908.

[16] WANG N, HE H K. Dynamics-level finite-time fuzzy monocular visual servo of an unmanned surface vehicle [J]. IEEE Transactions on Industrial Electronics, 2020, 67 (11): 9648−9658.

[17] DENG Q. High-precision tracking control of a quadrotor aircraft [D]. Dalian: Dalian Maritime University, 2019 (in Chinese).

[18] BHAT S P, BERNSTEIN D S. Finite-time stability of homogeneous systems [C]//Proceedings of the 1997 American Control Conference(Cat. No. 97CH36041). Albuquerque: IEEE, 1997: 2513−2514.

[19] SHTESSEL Y B, SHKOLNIKOV I A, LEVANT A. Smooth second-order sliding modes: missile guidance application [J]. Automatica, 2007, 43 (8): 1470−1476.

[20] FOSSEN T I. Guidance and control of ocean vehicles [M]. Chichester: Wiley, 1994.

[21] FENG Y, YU X H, MAN Z H. Non-singular terminal sliding mode control of rigid manipulators [J]. Automatica, 2002, 38 (12): 2159−2167.

[22] LIANG S. Research on the control system development and dynamic positioning of underwater detection and operation ROV [D]. Zhenjiang: Jiangsu University of Science and Technology, 2017 (in Chinese).

[23] WANG N, HE H K. Extreme learning-based monocular visual servo of an unmanned surface vessel [J]. IEEE Transactions on Industrial Informatics, 2020. doi: 10.1109/TII.2020.3033794.

[24] WANG N, SU S F. Finite-time unknown observer-based interactive trajectory tracking control of asymmetric underactuated surface vehicles [J]. IEEE Transactions on Control Systems Technology, 2021, 29 (2): 794−803.

[25] WANG N, Er M J. Self-constructing adaptive robust fuzzy neural tracking control of surface vehicles with

uncertainties and unknown disturbances [J]. IEEE Transactions on Control Systems Technology, 2015, 23 (3): 991−1002.

[26] WANG N, DENG Q, XIE G M, et al. Hybrid finite-time trajectory tracking control of a quadrotor [J]. ISA Transactions, 2019, 90: 278−286.

复杂扰动下水下机器人的轨迹精确跟踪控制

陈浩华[1], 赵红[1], 王宁[*1,2], 郭晨[1], 鲁挺[1], 王宁[1]

1 大连海事大学 船舶电气工程学院,辽宁 大连 116026

2 哈尔滨工程大学 船舶工程学院,黑龙江 哈尔滨 150001

摘　要:［**目的**］针对外界复杂干扰下水下机器人三维轨迹精确跟踪控制的问题,提出一种基于有限时间扰动观测器的非奇异终端滑模控制方法。［**方法**］设计非奇异终端滑模轨迹跟踪控制器,保证跟踪误差在有限时间内精确收敛到零。在外界多维度时变干扰下,设计有限时间扰动观测器,提高系统的抗干扰能力。［**结果**］利用Lyapunov 函数证明所设计控制策略可以有限时间稳定。采用MATLAB进行仿真实验,在阶跃扰动下与反步滑模控制方法仿真对比,表明所提方法可实现轨迹的精确跟踪。［**结论**］研究结果可为水下机器人的三维轨迹精确跟踪提供解决思路。

关键词: 水下机器人; 三维轨迹跟踪; 有限时间扰动观测器; 阶跃扰动; 非奇异终端滑模; 反步滑模